

WAVE-BLOCK IN EXCITABLE MEDIA DUE TO REGIONS OF DEPRESSED EXCITABILITY*

TIMOTHY J. LEWIS[†] AND JAMES P. KEENER[‡]

Abstract. We study propagation failure using the one-dimensional scalar bistable equation with a passive “gap” region. By applying comparison principles for this type of equation, the problem of finding conditions for block is reduced to finding conditions for the existence of steady state solutions. We present a geometrical method that allows one to easily compute the critical gap length above which a steady state solution, and thus block, first occurs. The method also helps to uncover the general bifurcation structure of the problem including the stability of the steady state solutions. In obtaining these results, we characterize the relationship between the properties of the system and propagation failure. The method can easily be extended to other gap dynamics. We use it to show that block associated with any local inhomogeneity must be associated with a limit point bifurcation.

Key words. inhomogeneous excitable media, propagation failure, super- and subsolutions

AMS subject classifications. 32C30, 92C30, 34B15, 35B40, 58F14

PII. S0036139998349298

1. Introduction. Spatially distributed excitable media appear in a wide range of physical systems including systems in population genetics, combustion dynamics, and physiology. Although most of these physical systems are inherently spatially inhomogeneous, they are often modeled as homogeneous media. This is despite the fact that the systems transmit signals via propagated waves of excitation and the interaction between the waves and inhomogeneities can have significant effects on the behavior of the waves. One important example is that regions with changes in excitability or conductivity can lead to stalling of the wave of excitation, thus blocking signal transmission, e.g., [11, 35, 12, 40]. This phenomenon is known as propagation failure or wave-block.

In this paper, we investigate wave propagation in an excitable medium with a localized region of low or no excitability and study the dynamical structure underlying wave-block. We refer to the region of reduced excitability as the “gap” and the entire model as the gap model. The gap model has a wide range of applications including problems from population genetics [9], chemical reaction theory [3], combustion theory [38], calcium-induced calcium release in muscle cells [36], extracellular signaling in glial cells [13], and electrical signaling in injured neurons [33]. However, our primary motivation for studying this situation originates from problems concerning the propagation of electrical excitation in cardiac tissue.

Although the majority of heart tissue is composed of electrically excitable cells that are well coupled, in both normal and pathological situations, waves of excitation in the heart encounter regions of depressed excitability. For instance, the atrioventricular (AV) node, which is the normal electrical pathway between the atria and

*Received by the editors December 11, 1998; accepted for publication (in revised form) October 21, 1999; published electronically July 19, 2000. This research was supported in part by NSF grant DMS 9626334.

<http://www.siam.org/journals/siap/61-1/34929.html>

[†]Department of Mathematics, University of Utah, Salt Lake City, UT, 84112. Current address: Center for Neural Science and Courant Institute for Mathematical Science, New York University, 4 Washington Place Rm 809, New York, NY, 10003 (tlewis@cims.nyu.edu).

[‡]Department of Mathematics, University of Utah, Salt Lake City, UT, 84112 (keener@math.utah.edu).

ventricular myocardium, is a localized region of low excitability and conductivity [20]. Waves of excitation originate at the sinus node, which is located in the right atrium. Normally, these waves are slowly, but successfully, transmitted through the AV node, but subtle changes can lead to propagation failure in the AV node. This is manifested as AV nodal arrhythmias (e.g., Wenckebach arrhythmias and AV nodal dissociation) [5, 21]. Also, heart attacks can lead to a localized region of ischemic or infarcted tissue in which excitability is substantially reduced. The interaction of waves of excitation and the structures mentioned above can lead to arrhythmias which involve wave-block. This block can be important in itself, but it can also trigger the onset of fatal reentrant arrhythmias (e.g., ventricular tachycardia and fibrillation) [27, 39].

The gap model is an idealized model for both the AV node and infarcted or ischemic regions. Indeed, the model under study is closely related to an experimental preparation, known as the sucrose gap preparation, which has been used to model the above situations [17, 34]. When recovery dynamics are included the gap model can exhibit all major behavior seen in the sucrose gap model (i.e., wave-block, Wenckebach rhythms, and reflection) [27]. Here, we consider only dynamics of excitation and therefore deal only with wave-block.

Specifically, we study the bistable reaction-diffusion equation with a “gap” region

$$(1.1) \quad u_t = (d(x)u_x)_x + h(u, x),$$

where the functions d and h are defined piecewise as follows:

$$d(x) = \begin{cases} D, & 0 \leq x < L, \\ 1 & \text{otherwise,} \end{cases}$$

and

$$h(u, x) = \begin{cases} g(u, x), & 0 \leq x < L, \\ f(u) & \text{otherwise.} \end{cases}$$

The function f describes local excitation outside the gap and the function g describes local dynamics in the gap. In the examples provided, the reaction term f is idealized to be the cubic function

$$f(u) = u(1-u)(u-\alpha), \quad 0 < \alpha < \frac{1}{2}.$$

However, it should be noted that the results directly apply to the standard, more general case $f \in C^1(R)$ satisfying

$$(1.2) \quad \begin{aligned} f(0) = f(\alpha) = f(1) = 0, & \quad 0 < \alpha < 1, \\ f(u) < 0, & \quad 0 < u < \alpha, \\ f(u) > 0, & \quad \alpha < u < 1, \\ f'(0) \neq 0 \neq f'(1), & \\ \int_0^1 f(u) \, du > 0. & \end{aligned}$$

Our main concern here is with the existence, stability, and bifurcation properties of specific nonuniform steady states of equation (1.1). These solutions act as time-independent supersolutions, and therefore their existence guarantees wave-block [30]. Generally, we use gap length L as the bifurcation parameter and determine the minimal gap length for which block occurs. We also describe properties of the steady state solutions that underlie wave-block. The reaction term in the gap, g , is taken

to be 0 for the bulk of the paper, corresponding to solely diffusion within the gap. However, other gap dynamics, as well as variations in parameters other than L , are considered.

The problem in which $g = 0$ has recently been studied by Sneyd and Sherratt [36] in the context of calcium-induced calcium release. However, they only briefly consider the special case of a piecewise linear discontinuous reaction term f and give only a preliminary analysis. On the other hand, in the context of population genetics, Fife and Peletier [9] consider a more general case. They model gap dynamics as a region with a decreased nonuniform reaction term, and using super- and subsolution techniques, they obtain necessary conditions for the existence of stable steady state solutions. By considering a special case of the Fife and Peletier problem and a more general case of Sneyd and Sherratt, we are able to extend their results.

Wave-blocking phenomena have been studied along these lines for various other inhomogeneities. Propagation failure has been examined via the existence of nonuniform steady states in media with periodically varying diffusion coefficients and/or excitability [38, 24, 37], as well as in discrete bistable systems [23, 7]. Other studies have determined conditions for the existence of nonuniform steady states in media that have an abrupt increase in diffusion coefficient (equivalent to an increase in cable diameter or a branched cable) [30, 16, 9]. Because the latter studies involve media with a local inhomogeneity, they are more relevant to the present study. Indeed, although quite different in the technical details, our work parallels the work of Pauwelussen [30]. Pauwelussen analytically obtains a precise value for the critical increase in the diffusion coefficient above which “blocking” steady states exist (see also Fife and Peletier [9]), yet he also provides a geometrical interpretation in which overlapping phase planes are used to piece together the invariant manifolds that constitute the steady state solutions. This geometrical interpretation reveals the bifurcation structure of the problem and helps to render super- and subsolutions which give the stability of the steady states.

The gap problem is more complex than the problem with an abrupt increase in diffusion coefficient. Precise analytical conditions for block cannot be obtained [9] even for the simplest gap dynamics, $g = 0$. However, by a novel combination of shooting arguments and a geometrical idea similar to that of Pauwelussen, we are able to gain considerable insight into the underlying dynamical structure of the problem. This geometric approach provides a simple computational method to determine critical conditions for the existence of steady state solutions (and wave-block). It also provides a way to easily construct the steady state solutions and determine properties of these solutions. Furthermore, as in Pauwelussen’s work, our geometrical interpretation aids in constructing sub- and supersolutions from which stability of the steady states is obtained.

The behavior of equation (1.1) is similar to the behavior found in the system with the increase in diffusion coefficient, especially with respect to the bifurcation structure. Steady state solutions arise from a limit point bifurcation. Specifically, the stability properties of the solutions are indicative of a saddle-node bifurcation. In fact, our geometrical method can be generalized to show that block due to any local inhomogeneity must be associated with this type of bifurcation.

The paper is organized as follows. In section 2, we study the case where gap dynamics are governed purely by diffusion. We describe the link between nonuniform steady state solutions and wave-block and present a geometric method for determining the existence of steady states of equation (1.1). We then show how this geometric

idea allows one to determine properties of the solutions, including their stability. In an attempt to show how these results fit into a larger framework, the connection to coupled cells is presented in section 3. This leads to the consideration of other gap dynamics for equation (1.1) in section 4. In section 5, we review our results and discuss the limitations of their applicability.

2. The strictly diffusive gap. In this section, gap dynamics are taken to be strictly diffusive, $g = 0$. This is the simplest possible case for system (1.1), but it allows for the development of concepts that can be used for the more complicated cases considered in section 4. Also, the qualitative results for the strictly diffusive case carry over to the other cases.

2.1. Wave propagation and wave-block. Before addressing the problem of how inhomogeneities affect signal propagation in a one-dimensional bistable system, let us first consider the case of a uniform cable (equation (1.1) with $L = 0$). In the absence of any inhomogeneities, signal transmission occurs as a propagated wavefront of excitation that can be realized mathematically as a traveling wave solution. This solution is of the form $u(x, t) = U(x + ct - \xi)$ with arbitrary ξ (translation invariance) and provides a transition between the resting state $u = 0$ and the excited state $u = 1$ such that $0 \leq U \leq 1$ with $U(\infty) = 1$, $U(-\infty) = 0$ and $U_x(\pm\infty) = 0$. The parameter c is the speed of the traveling wavefront and is determined by the reaction term f . A proof for the existence of this traveling wave was first given by Aronson and Weinberger [1], who also showed that U is strictly increasing and that the wave speed c is positive for $\int_0^1 f(u)du > 0$. Fife and McLeod [8] later showed that the traveling wave is stable, and if

$$\limsup_{x \rightarrow -\infty} u(x, 0) < \alpha, \quad \liminf_{x \rightarrow \infty} u(x, 0) > \alpha,$$

where α is defined as in conditions (1.2), then the solution $u(x, t)$ approaches $U(x + ct - \xi)$ exponentially, for some ξ as $t \rightarrow \infty$.

If the gap length L is nonzero but small, then although there is no true traveling wave, one would expect that the dynamics would behave similarly to the uniform case. Indeed, numerical simulations confirm this. When a wavefront propagating towards the gap reaches the proximal side of the gap, it stalls because there is no excitability in the gap. However, it begins to feed u to the distal side of the gap via diffusion. For small L , the wavefront is able to supply enough u to excite the distal side of the gap. Thus, after a slight delay, the wavefront is able to jump the gap. In fact, the solution exponentially approaches the traveling wave solution for the uniform cable $u(x, t) = U(x + ct - \xi)$ as $t \rightarrow \infty$. (The proof of this is virtually identical to that in [30], which is for the case of a single abrupt change in cable diameter.)

As L is increased, the delay increases, but the wavefront is still able to jump the gap. This behavior continues until L is increased above a critical value, L^* , after which the wavefront completely stalls. For these “large” values of L , the solution appears to approach a nonuniform steady state solution and thus there is block.

Figure 2.1 shows examples of both successful transmission of the wavefront across the gap (top) and wavefront block (bottom). For these simulations, the excitability term f is taken to be cubic with $\alpha = 0.3$ and in the gap, $D = 1$. The critical gap length L^* is approximately 6.5 in this case. These simulations look strikingly similar to those of Sharp and Joyner [35] in which a detailed model for cardiac ventricular muscle is used.

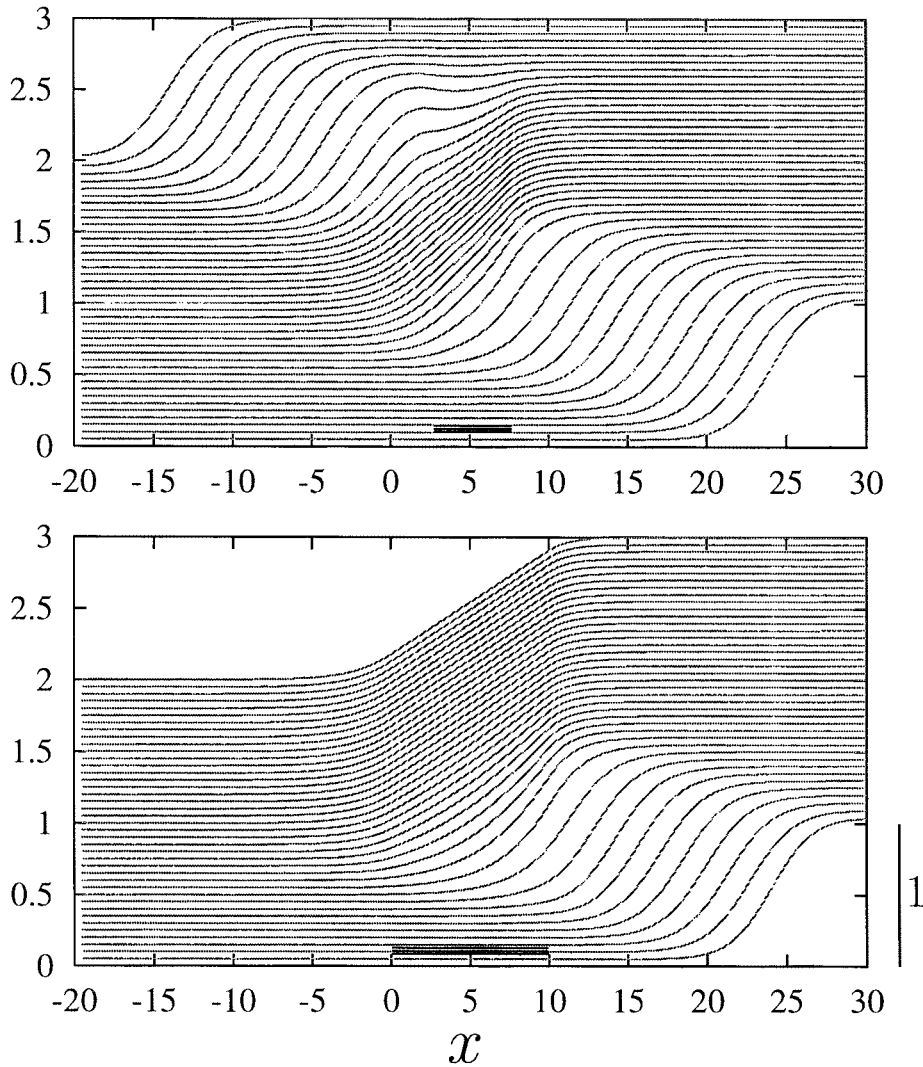


FIG. 2.1. Numerical simulations of equation (1.1) with $D = 1$, $\alpha = 0.3$. Plots are of u vs. space (x). Each curve is the solution at a fixed time (every 5 time units) and as time progresses the curves are lifted slightly. The position of the gap is marked by a black bar on each figure. The wavefront propagates towards the gap from the right. In the top figure, there is successful transmission across the gap ($L = 5.0$), whereas in the bottom figure, the wavefront is blocked ($L = 10.0$). These simulations were performed using an implicit-explicit method [14] with $\Delta t = 0.001$ and $\Delta x = 0.01$.

Long delays before successful jumping of the gap make it computationally intensive to get good estimates of L^* . Furthermore, obtaining anything more than a critical gap length for a specific excitability function at a specific set of parameters by doing numerical simulations of the full partial differential equation is difficult. For this reason, we turn to analytical methods to help us gain further insight into the problem at hand.

2.2. Steady state solutions and block. In the numerical simulations presented, it can be seen that, when block occurs, the solution appears to approach a

steady state in which the proximal side of the medium is in the excited state and the distal side is close to the resting state (see Figure 2.1). This points to the link between block and the existence of certain nonuniform steady states. This link is a result of comparison principles that are based on the maximum principle for scalar parabolic partial differential operators (see Protter and Weinberger [32]) and the concepts of super- and subsolutions. These comparison principles are due to Pauwelussen [30], who extended the landmark work of Aronson and Weinberger [1].

DEFINITION 1. *Suppose that $\phi \in C^{2,1}(R \setminus \{x_j, j = 1, \dots, N\} \times (0, \infty))$. $\phi(x, t)$ is a subsolution of equation (1.1), if $\phi_t - (d(x)\phi_x)_x - h(\phi, x) \leq 0$ on differentiable segments of ϕ and $d((x_j^+)\phi_x(x_j^+, t)) - d((x_j^-)\phi_x(x_j^-, t)) \geq 0$, where $d(x)\phi_x$ has discontinuities.*

$\phi(x, t)$ is a supersolution of equation (1.1), if $\phi_t - (d(x)\phi_x)_x - h(\phi, x) \geq 0$ on differentiable segments of ϕ and $d((x_j^+)\phi_x(x_j^+, t)) - d((x_j^-)\phi_x(x_j^-, t)) \leq 0$, where $d(x)\phi_x$ has discontinuities.

THEOREM 2 (comparison principle). *Let $\bar{\phi}(x)$ be a time-independent supersolution of equation (1.1) and $u(x, t)$ be the solution to equation (1.1) with the initial condition $\bar{\phi}(x)$. Then $u(x, t)$ is a nonincreasing function of t and approaches the largest steady state solution $u^*(x)$ of equation (1.1) such that $u^*(x) \leq \bar{\phi}(x)$. Similarly, Let $\underline{\phi}(x)$ be a time-independent subsolution of equation (1.1) and $u(x, t)$ be the solution to equation (1.1) with the initial condition $\underline{\phi}(x)$. Then $u(x, t)$ is a nondecreasing function of t and approaches the smallest steady state solution $u^*(x)$ of equation (1.1) such that $u^*(x) \geq \underline{\phi}(x)$.*

For a constant diffusion coefficient, this result follows directly from Aronson and Weinberger [1], since the spatial dependence of the reaction term does not affect the argument used to prove this ordering principle. When diffusion constant $d(x)$ varies but is continuous, the result is obtained directly following a change of variables. Furthermore, an extension of the theorem by Pauwelussen [30, 31] includes the case of discontinuities in the diffusion coefficient.

For our purposes, the link between the existence of nonuniform steady states and block can be summarized by the following proposition, which follows directly from the above theorem.

PROPOSITION 3. *Consider the system described by equation (1.1). A wavefront propagating towards the gap from the right ($x > L$) fails to cross the gap, if and only if a nonuniform steady state solution $u^*(x)$ of the equation (1.1) exists for which $u, u_x \rightarrow 0$ as $x \rightarrow -\infty$ and $u \rightarrow 1, u_x \rightarrow 0$ as $x \rightarrow \infty$. If such a steady state exists, the solution asymptotically approaches this steady state (or a similar, but smaller, nonuniform steady state), and hence the wavefront is blocked. If no such steady state exists, the solution approaches $u = 1$, the smallest steady state greater than the initial conditions, and hence the wavefront successfully jumps the gap.*

2.3. Steady state solutions: A geometrical approach. The above argument reduces the problem of looking for wave-block to simply looking for steady state solutions, $u(x)$ [30]. (For convenience, the * superscript denoting steady state solutions is dropped and steady state solutions are simply referred to as u or $u(x)$. The time-dependent solutions to the full partial differential equation are referred to explicitly as $u(x, t)$.) The steady state solutions must satisfy the boundary value problem

$$(2.1) \quad 0 = \begin{cases} u_{xx} + f(u), & x \in (-\infty, 0), \\ Du_{xx}, & x \in (0, L), \\ u_{xx} + f(u), & x \in (L, \infty), \end{cases}$$

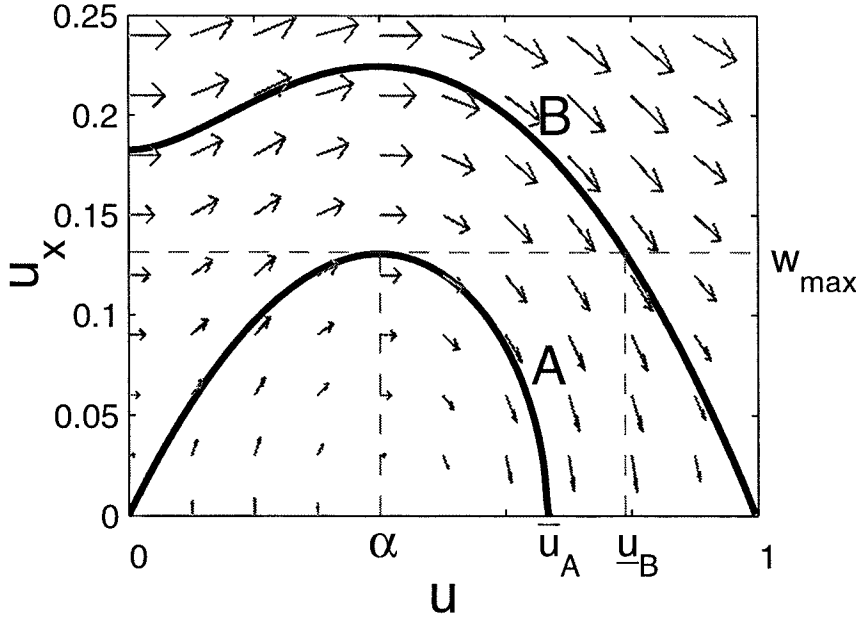


FIG. 2.2. The u, u_x -phase portrait of $u_{xx} + f(u) = 0$ with vector field. f is cubic with $\alpha = 0.4$. Curve A is the homoclinic orbit associated with $(0, 0)$ and curve B is the stable manifold of $(1, 0)$.

with the boundary conditions mentioned above. Also, matching conditions must be satisfied for u (continuity) and for u_x (the jump condition or conservation of current)

$$\begin{aligned} \lim_{x \rightarrow 0^-} u &= \lim_{x \rightarrow 0^+} u, & \lim_{x \rightarrow 0^-} u_x &= \lim_{x \rightarrow 0^+} Du_x, \\ \lim_{x \rightarrow L^+} u &= \lim_{x \rightarrow L^-} u, & \lim_{x \rightarrow L^+} u_x &= \lim_{x \rightarrow L^-} Du_x. \end{aligned}$$

To a limited extent, this problem can be addressed algebraically [36]. However, we find that it is much more enlightening to consider a geometrical interpretation of the problem. This interpretation mixes the idea of piecing flows in phase planes together (similar to Pauwelussen [30], see also [22]) and the idea of shooting [25].

Consider the phase portrait of $u_{xx} + f(u) = 0$ shown in Figure 2.2. Two important trajectories are plotted in the phase plane: curve A is a portion of the homoclinic orbit emanating from the saddle point $((u, u_x) = (0, 0))$ and curve B is the stable manifold of the saddle point $((u, u_x) = (1, 0))$. Note that on trajectory A, $u, u_x \rightarrow 0$ as $x \rightarrow -\infty$. This is exactly the left boundary condition of steady state equation (2.1). On trajectory B, $u \rightarrow 1, u_x \rightarrow 0$ as $x \rightarrow \infty$, which is the boundary condition on the right. Thus, we see that the steady state solution $u(x)$ to the left of the gap ($x \leq 0$) lives on trajectory A, and therefore so does $(u(0), u_x(0))$. Similarly, $u(x)$ to the right of the gap ($x \geq L$) lives on trajectory B, and therefore so does $(u(L), u_x(L))$.

Next, we note that the flow in the gap (on $0 < x < L$) is governed by the differential equation $Du_{xx} = 0$. Let us take points on curve A to be a family of initial conditions ($x = 0$) and flow forward using this differential equation to $x = L$. If any trajectory stemming from a point on A, say point a , matches up with a point on curve B, say point b , then we have found a solution to the steady state equation (2.1). This solution can be reconstructed by considering the (u, u_x) coordinates and tracing out the following trajectory in the phase plane. Starting at $(0, 0)$ ($x = -\infty$), move along

curve A to point a . Because curve A is a homoclinic orbit, the x value is arbitrary at this point, so we can set it to $x = 0$. From point a , follow the flow of $Du_{xx} = 0$, which is horizontal in the u_x, u -phase plane (u_x constant), until $x = L$. By design this is point b on curve B . The remaining portion of the solution is obtained by following curve B , the stable manifold of $(1,0)$, into the steady state $(1,0)$ while x increases from L to ∞ .

The description above suggests an easy way to find steady state solutions. As before, consider points on curve A as all possible $x = 0$ values for our solution. We can derive a map by the flow in the gap ($Du_{xx} = 0$) and map these points on curve A , $(u(0), u_x(0))$, to points on a new curve $\psi_L(A)$

$$\psi_L : [u(0), u_x(0)] \mapsto \left[u_x(0) \frac{L}{D} + u(0), u_x(0) \right].$$

Any intersection of this new curve $\psi_L(A)$ and curve B corresponds to a steady state solution of the partial differential equation (1.1).

The map ψ_L is continuous and has fixed points where $u_x = 0$, which occurs at two points along the trajectory A . When $L = 0$, the map is the identity map, so curve $\psi_L(A)$ is exactly curve A . When L is positive, the map effectively shifts points on curve A to the right (towards trajectory B) for $u_x > 0$. The map shifts curve A to the left (away from trajectory B) for $u_x < 0$, thus no intersections can occur on this portion of A . The shift is linear in L and the greater u_x is, the larger the shift.

Note that the bifurcation parameter of interest here can be thought of as L/D , therefore usually we take $D = 1$ in what follows without loss of generality.

2.4. Results: Existence and properties of solutions. An example of the mapping described in the previous section is given for the cubic f with $\alpha = 0.3$ in Figure 2.3. One can see that for small L , there are no intersections of $\psi_L(A)$ and curve B . However, as L increases, a critical value of L , L^* , is reached where there is one intersection, and thus one steady state solution to equation (1.1). For L greater than this critical value, two intersections, and thus two steady state solutions, exist. This implies that the solutions arise via a limit point bifurcation. A bifurcation diagram for this system is shown in Figure 2.4. This bifurcation structure is similar to that found in the case of an abrupt change in diffusion coefficient [30, 16]. However, in the next section, we show that more than two solutions can arise in the gap problem, which is not the case for the abrupt change in diffusion coefficient. Figure 2.5 shows an example of steady state solutions of equation (1.1) for $L > L^*$. These solutions were constructed using the values at the intersection points in Figure 2.3.

An interesting aspect of this graphical representation is that it immediately shows the portions of the reaction term f that determine whether or not block occurs. The maximal value that u attains on curve A is \bar{u}_A , where \bar{u}_A is defined by $\int_0^{\bar{u}_A} f(u) du = 0$. Also, curve A attains a maximal value of u_x , w_{\max} , when $u = \alpha$, i.e., $w_{\max} = \sqrt{-2 \int_0^\alpha f(u) du}$. A steady state solution lives on curve A on the distal side of the gap, therefore $0 \leq u \leq \bar{u}_A$ on this side. Furthermore, because points on curve A are mapped horizontally in the u, u_x -phase plane by ψ_L , w_{\max} is the maximal value of u_x that a steady state solution can attain. A steady state solution on the proximal side of the gap lives on curve B , and thus $\underline{u}_B \leq u \leq 1$ on the proximal side of the gap, where \underline{u}_B is the value of u on curve B associated with $u_x = w_{\max}$, i.e., $w_{\max} = \sqrt{2 \int_{\underline{u}_B}^1 f(u) du}$. This leaves the interval $u \in (\bar{u}_A, \underline{u}_B)$ and the corresponding portion of f unrepresented in the excitable region for all L . (Note that α , w_{\max} , \bar{u}_A , and \underline{u}_B are shown in Figure 2.2.)

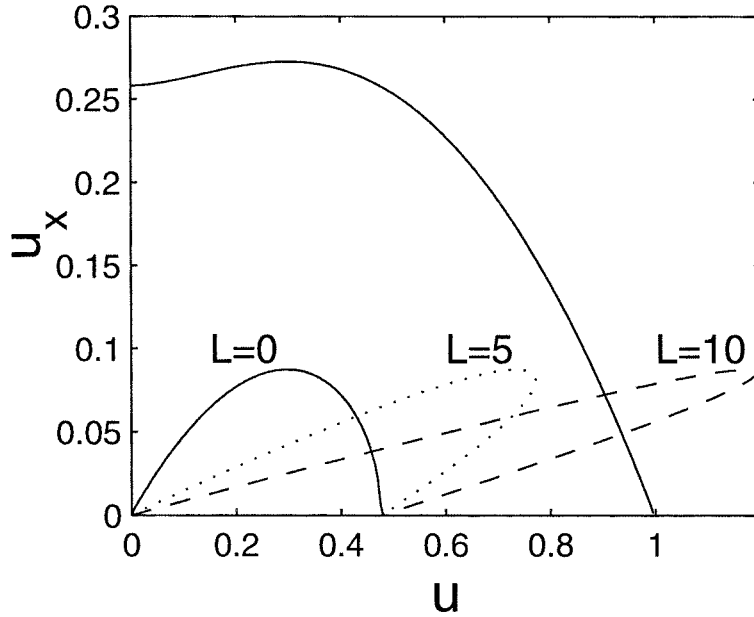


FIG. 2.3. u, u_x -phase portrait of $u_{xx} + f(u) = 0$ (as in previous figure) with images of the homoclinic orbit (curve A) under the map ψ_L . Intersections with the stable manifold of $(1, 0)$ (curve B) correspond to steady state solutions of equation (1.1). $\alpha = 0.3, D = 1$. The first intersection is at $L^* = 6.40$.

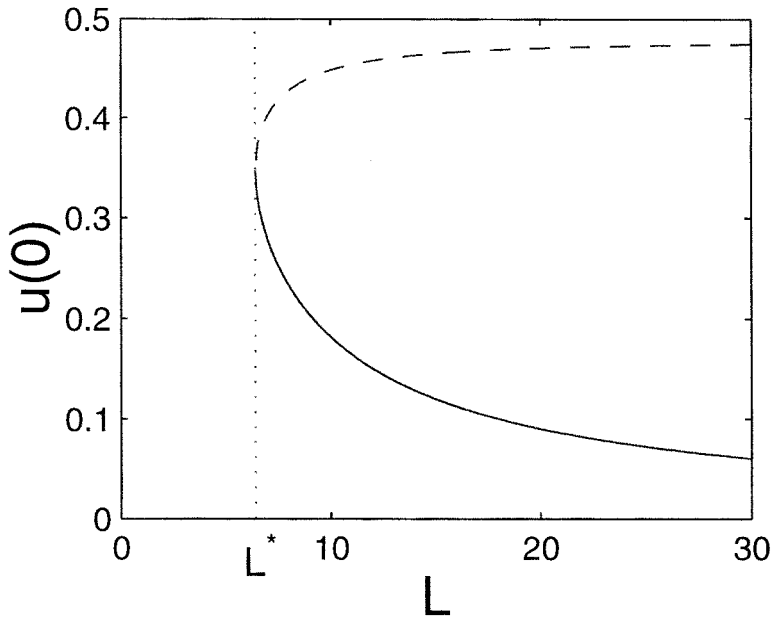


FIG. 2.4. Bifurcation diagram: $u(0)$ of the steady state solution vs. gap length (L). The solid line represents stable solutions and the dashed line represents unstable solutions. The critical gap length is $L^* = 6.40$. The parameters are $\alpha = 0.3, D = 1$.

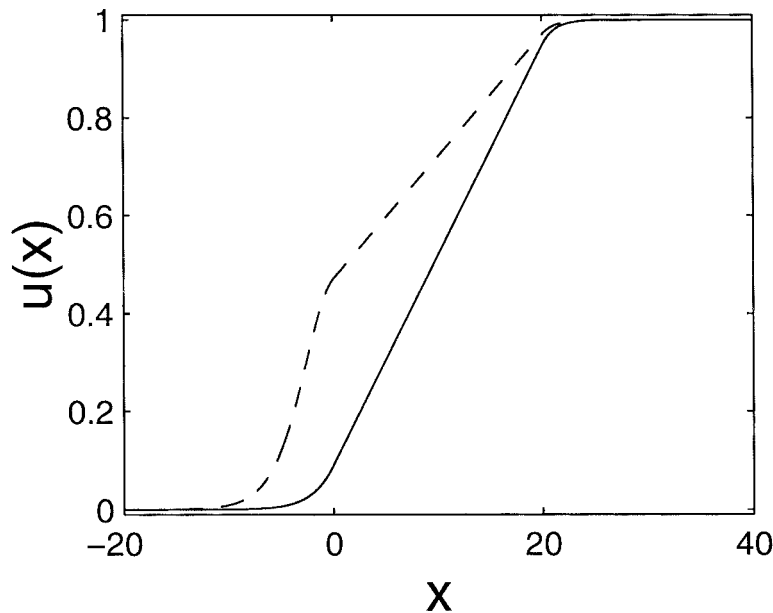


FIG. 2.5. The steady state solutions of equation (1.1) for $L = 20.0$. The solid line represents the stable solution and the dashed line represents the unstable solution. Parameters are $\alpha = 0.3$, $D = 1$.

For instance, for $\alpha = 0.3$, we can see in Figure 2.3 that the values of f for $u \in (0.5, 0.9)$ are inconsequential with respect to possible steady states and therefore whether there is block or not. That is, two different reaction terms f that are the same on $0 < u < 0.5$ and $0.9 < u < 1.0$ could be extremely different between 0.5 and 0.9, yet the corresponding gap problem would exhibit an identical L^* and the same steady state solutions for $L \geq L^*$. Note that as α decreases, the size of this “inconsequential” region increases substantially.

Figure 2.6 shows the critical gap length as a function of the threshold parameter α . As intuition would predict, the critical gap length L^* decreases as α increases. $L^* = 0$ at $\alpha = 0.5$, which corresponds to a standing wave in the homogeneous cable. As α approaches 0 from above, L^* goes to ∞ . The $\alpha = 0$ case corresponds to a Fisher-like equation [10] where the slightest perturbations away from the resting state leads to traveling wavefronts, thus for any finite gap length and nonzero diffusion in the gap, wavefronts are able to jump the gap.

By using the geometric interpretation of the problem, we can now extend and solidify the ideas generated from the example above and easily prove the following existence proposition.

PROPOSITION 4. *Consider the steady state scalar gap problem (2.1) with $L \geq 0$. There exists a critical value L^* such that the system has no solutions for $L < L^*$, exactly one solution at $L = L^*$ (generically), and at least two solutions for $L > L^*$. Furthermore, solutions arise or disappear via limit point bifurcations.*

By our restrictions on f , there is a homoclinic orbit, curve A , which is associated with $(0, 0)$. For $u_x = w > 0$, it lies entirely below the stable manifold of $(1, 0)$, curve B . Thus, because the map ψ_L is the identity map for $L = 0$, there are no intersections of curve B and $\psi_L(A)$, and therefore no solution to the system exists.

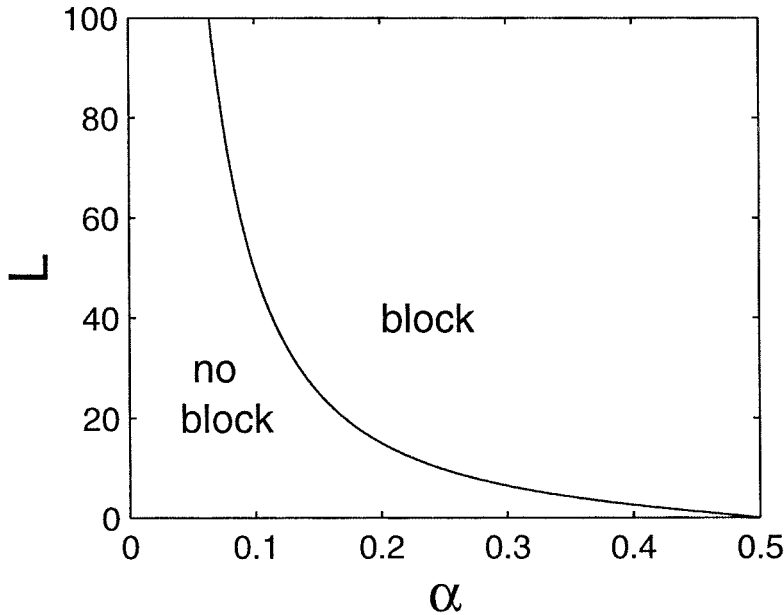


FIG. 2.6. Critical gap length L^* vs. α for a cubic reaction term. This curve plots the locus of the fold (see Figure 2.4), as the parameter α is changed. The curve was calculated using AUTO [6].

The map ψ_L shifts points (u, u_x) on curve A such that the u_x values remain unchanged and u values are increased by the amount $u_x L$. That is, for fixed u_x , ψ_L maps u values of points on A in a monotonic (linear) fashion with respect to L . This mapping is therefore strictly increasing for $u_x > 0$, while points with $u_x = 0$ remain fixed. Thus, $\psi_L(A)$ intersects B for sufficiently large L with $u_x > 0$.

The monotonicity of ψ_L in L , the continuity of ψ_L , and the continuity of the curves A and B ensures that, as L increases, the first crossing must be tangential. Generically, this occurs at a single point. Let us define L to be L^* at this critical value. The above properties also guarantee that at least two nontangential intersections exist for $L > L^*$. The existence of solutions to equation (2.1) follow from the existence of these intersection points.

The following proposition lists some properties of the steady state solutions.

PROPOSITION 5. *The steady state solutions of the scalar gap problem (2.1) have the following properties:*

- (i) *Solutions are monotonically increasing ($u_x > 0$).*
- (ii) *Solutions have bounds $0 < u_x \leq w_{\max}$, $0 < u(0) < \bar{u}_A$, and $\underline{u}_B \leq u(L) < 1$.*
- (iii) *For a given L , steady state solutions are nowhere equal (i.e., they are ordered).*
- (iv) *There exists an L^{**} such that there are exactly two solutions for $L > L^* > L^{**}$.*
- (v) *There exists a solution $u(x)$ such that $u(0) = \alpha$ for some $L > L^*$. (This $L > L^*$ is often a good estimate of the critical gap length.)*

These properties are fairly easily seen by inspecting of the phase plane and briefly considering of the mapping of curve A . Therefore, the proofs for Proposition 5 are not given here; the proofs can be found in [27].

2.5. The appearance and disappearance of solutions. To acquire more information about the appearance and disappearance of solutions, we consider the

bifurcation structure of system (2.1) in more detail. This standard bifurcation analysis is included because it allows us to obtain a relationship that helps us to analytically determine the stability of solution branches.

Let $w = u_x$ and $w = G_A(u) = \sqrt{-2 \int_0^u f(v) dv}$ describe the homoclinic orbit A for $w > 0$ on $u \in (0, \bar{u}_A)$ (refer to Figure 2.2). $G_A(u)$ is strictly decreasing on $u \in (\alpha, \bar{u}_A)$, and thus can be inverted on this region, $u = G_A^{-1}(w) = U_A(w)$. Similarly, $w = G_B(u) = \sqrt{2 \int_u^1 f(v) dv}$, and therefore $u = G_B^{-1}(w) = U_B(w)$, describes the decreasing portion of the stable manifold of $(1, 0)$, curve B with $u \in (\alpha, 1)$. We can now express the map ψ_L as

$$\psi_L : [U_A(w), w] \mapsto [wL + U_A(w), w]$$

and look for solutions to

$$wL + U_A(w) = U_B(w),$$

where w is $u_x(0)$ on a solution of equation (2.1). Rearranging this equation, we obtain

$$(2.2) \quad H(w; L) = U_A(w) + wL - U_B(w) = 0.$$

Assume that we know a solution $u(x)$ of equation (2.1) for $L = L_0$ with $u_x(0) = w_0$. Then

$$(2.3) \quad H(w_0; L_0) = U_A(w_0) + w_0 L_0 - U_B(w_0) = 0.$$

By expanding H in a Taylor series about $(w_0; L_0)$ and using the above equation, we get

$$\begin{aligned} H(w; L) &= [U'_A(w_0) + L_0 - U'_B(w_0)](w - w_0) + w_0(L - L_0) \\ &\quad + [U''_A(w_0) - U''_B(w_0)](w - w_0)^2 + (w - w_0)(L - L_0) + H.O.T. \\ &= 0. \end{aligned}$$

Thus, bifurcations can occur when

$$(2.4) \quad U'_A(w_0) + L_0 - U'_B(w_0) = 0.$$

Note that it is required that $U'_A(w_0) < 0$ in order to have solutions to this equation, because L_0 and $-U'_B(w_0)$ are both positive. This is always the case for the branch of curve A that we have chosen to work with, however it is never the case on the $u \in (0, \alpha)$ branch of curve A , i.e., all bifurcations occur with $u(0) > \alpha$.

By using (2.3) and (2.4), we have two equations for the two unknowns w_0 and the value of L at the bifurcation point. Solving these equations for L_0 , we get

$$(2.5) \quad L_0 = -U'_A(w_0) + U'_B(w_0) = -\frac{1}{w_0}[U_A(w_0) - U_B(w_0)].$$

To find the type of bifurcation algebraically, we let

$$L = L_0 + \epsilon L_1 + \epsilon^2 L_2 + \dots,$$

$$w = w_0 + \epsilon w_1 + \epsilon^2 w_2 + \dots,$$

where ϵ is a small positive parameter, and substitute into (2.2) and collect like terms. The $O(\epsilon)$ equation is

$$w_0 L_1 = 0,$$

which implies that $L_1 = 0$. The $O(\epsilon^2)$ terms give

$$w_0 L_2 + w_1^2 [U_A''(w_0) - U_B''(w_0)] + L_1 w_1 = 0.$$

L_2 is arbitrary and we can choose it to give the direction of the perturbation away from the bifurcation point. If we choose $L_2 = +1$, then

$$w_1 = \pm \sqrt{\frac{-w_0}{U_A''(w_0) - U_B''(w_0)}},$$

which exists when $U_A''(w_0) - U_B''(w_0) < 0$. This implies that if there is a bifurcation at $L = L_0$, then two new solutions are born as L is increased. If we choose $L_2 = -1$, then

$$w_1 = \pm \sqrt{\frac{-w_0}{-U_A''(w_0) + U_B''(w_0)}},$$

which exists when $U_A''(w_0) - U_B''(w_0) > 0$. This implies that if there is a bifurcation at $L = L_0$, then two solutions coalesce at $L = L_0$ and vanish as L is increased. In the nongeneric case that $U_A''(w_0) - U_B''(w_0) = 0$, higher-order terms must be considered to ascertain what happens.

The above gives a condition for the existence of more than two solutions: If $U_A''(w) - U_B''(w)$ changes sign on $u \in (\alpha, \bar{u}_A)$, then more than two solutions can exist. In fact, the number of sign changes determines the number of possible limit point bifurcations, and thus the number of solutions that can possibly coexist. If $U_A''(w) - U_B''(w)$ does not change sign, then there is a single bifurcation and a maximum of two solutions. This is the case for the cubic f as shown in Figures 2.3 and 2.4. Figure 2.7 shows the phase portrait with mapping of curve A for the case of $f = -u(u - 0.17)(u - 1.0)(u^2 - 1.1u + 0.3075)$ in which $U_A''(w) - U_B''(w)$ changes sign twice. As a result of these sign changes, three bifurcations occur: two saddle-node bifurcations in which two solutions are born in each and one where the middle two solutions coalesce and vanish. This leads to a maximum of four steady state solutions.

Note that at a bifurcation point where two solutions are born as L is increased

$$H_w(w_0; L_0) = [U_A'(w_0) - U_B'(w_0)] + L_0 = 0$$

and

$$H_{ww}(w_0; L_0) = U_A''(w_0) - U_B''(w_0) < 0.$$

Thus by continuity and ordering, the solution branch with $w < w_0$ immediately following the bifurcation point, and thus the “greater” solution because $w = G_B(u)$ is monotonically decreasing in u in the pertinent region, has

$$(2.6) \quad U_A'(w_0) - U_B'(w_0) + L_0 > 0.$$

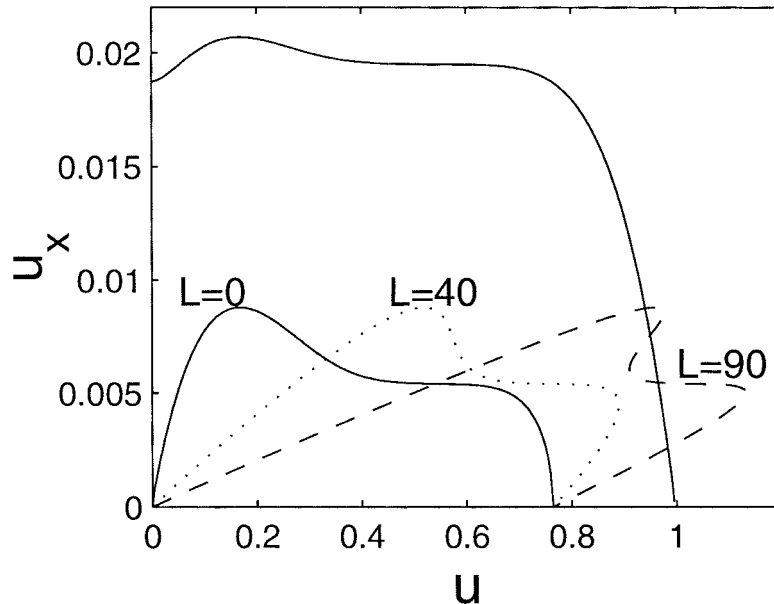


FIG. 2.7. The u, u_x -phase portrait of $u_{xx} + f(u) = 0$ with images of the homoclinic orbit (curve A) under the map ψ_L . Here, a quintic reaction term is used $f = -u(u - 0.17)(u - 1.0)(u^2 - 1.1u + 0.3075)$. At $L = 90$, it can be seen that there are four intersections of the mapped homoclinic orbit A and the stable manifold of $(1, 0)$ (curve B). These intersections correspond to four steady state solutions of equation (1.1).

The solution branch with $w > w_0$ immediately following the bifurcation point, and thus the “smaller” solution, has

$$(2.7) \quad U'_A(w_0) - U'_B(w_0) + L_0 < 0.$$

In the next section, these conditions are used to show that the smaller solution is stable and the larger solution is unstable. The stability of one branch and the instability of the other is exactly what we expect from a saddle-node bifurcation. Note that one can justify the above result graphically as well.

2.6. Stability of solutions. Stability of the solutions can be determined by numerical simulations of (1.1) (i.e., observing dynamics for small perturbations away from steady states $u(x)$) or by linearizing around $u(x)$ and calculating the eigenvalues of the resulting Schrödinger-type equation. However, these results would only be applicable to the general case in an inferential way. Here, we show stability for general f .

The following proposition implies that, any time two new solutions are born, the larger solution is unstable and the smaller is stable. We show this by constructing time-independent super- and subsolutions that are solutions of (1.1) everywhere except at $x = 0$. Therefore, they live on curve A for $x < 0$, they are straight lines on $0 < x < L$, they live on curve B for $x > L$, and have continuous second derivatives everywhere but $x = 0$ where a jump in the x -derivative occurs. Conditions for the existence of these super- and subsolutions give us our result.

PROPOSITION 6. Let $u(x)$ be a steady state solution of (1.1).

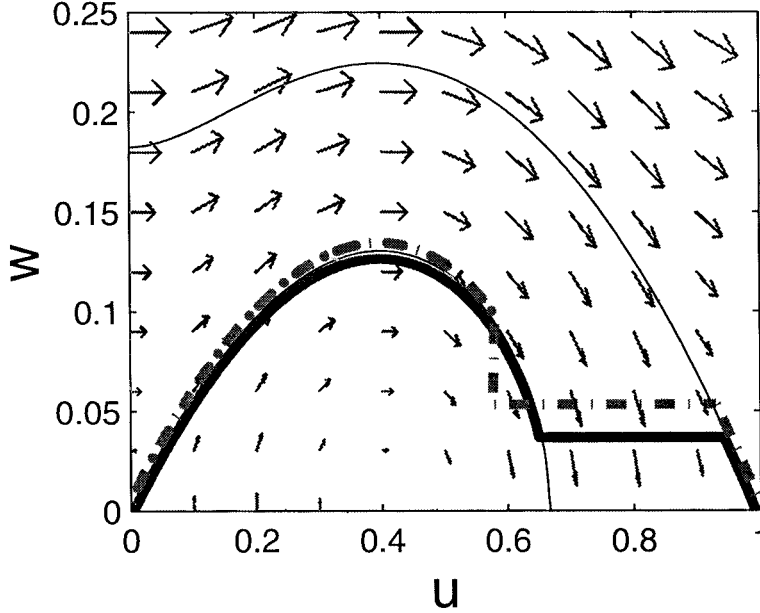


FIG. 2.8. Phase plane for cubic f with $\alpha = 0.4$. The trajectory for a steady state solution u^* of equation (1.1) is plotted as a thick solid line. The trajectory for a time-independent supersolution $\bar{\phi}$ is plotted as a thick dot-dashed line. ($D = 1, L = 7.2$). Values of interest: $u^*(0) = 0.650$, $u^*(L) = 0.942$, $u_x^*(0) = u_x^*(L) = 0.041$. $\bar{\phi}(0) = 0.576$, $\bar{\phi}(L) = 0.930$, $\bar{\phi}_x(0+) = \bar{\phi}_x(L) = 0.051$ (i.e., $\epsilon = 0.1$), $\bar{\phi}_x(0-) = 0.0939$, $U_A(\bar{\phi}_x(0+)) \sim 0.64$.

(i) If $U'_A(u_x(0)) - U'_B(u_x(0)) + L < 0$, then there exists a time-independent supersolution $\bar{\phi}(x)$ and subsolution $\underline{\phi}(x)$ that are arbitrarily close to $u(x)$ with $\bar{\phi}(x) > u(x) > \underline{\phi}(x)$. Therefore, $u(x)$ is a stable solution.

(ii) If $U'_A(u_x(0)) - U'_B(u_x(0)) + L > 0$, then there exists a time-independent supersolution $\bar{\phi}(x)$ and subsolution $\underline{\phi}(x)$ that are arbitrarily close to $u(x)$ with $\bar{\phi}(x) < u(x) < \underline{\phi}(x)$. Therefore, $u(x)$ is an unstable solution.

In constructing a supersolution with $\bar{\phi}(x) < u(x)$, it is extremely useful to follow its trajectory in the phase plane shown in Figure 2.8. Let us attempt to build the supersolution starting from $x = \infty$ and then decreasing x to $x = -\infty$. From $x = L$ to ∞ , take $\bar{\phi}$ to live on curve B with $\bar{\phi}'(L) = u_x(L) + \epsilon$, where ϵ is arbitrarily small. Because curve B is monotonic with $U'_B < 0$ in the region of interest, it is required that $\epsilon > 0$ in order to have $\bar{\phi}(x) < u(x)$. For $0 < x < L$, take $\bar{\phi}$ to be a straight line such that $\bar{\phi}$ and $\bar{\phi}'$ are continuous at $x = L$. The equation for $\bar{\phi}(0)$ is then

$$\bar{\phi}(0) = -(u_x(L) + \epsilon)L + U_B(u_x(L) + \epsilon).$$

The remainder of $\bar{\phi}$ is taken to live on curve A with $\bar{\phi}$ continuous. Thus, $\bar{\phi}$ is a solution everywhere except $x = 0$ where generically $\bar{\phi}'$ is not continuous (for $\epsilon \neq 0$). For $\bar{\phi}$ to be a supersolution, the jump condition $\bar{\phi}'(0+) - \bar{\phi}'(0-) < 0$ must be satisfied. Therefore, it is required that $\bar{\phi}(0) < U_A(u_x(L) + \epsilon)$ for points with $u \in (\alpha, \bar{u}_A)$ where $U'_A < 0$ (or $\bar{\phi}(0) > U_A(u_x(L) + \epsilon)$ for points with $u \in (\alpha, \bar{u}_A)$, where $U'_A > 0$). This gives the inequality

$$-(u_x(L) + \epsilon)L + U_B(u_x(L) + \epsilon) < U_A(u_x(L) + \epsilon).$$

Expanding the inequality in a Taylor series about $\epsilon = 0$ and collecting like terms, we get

$$(U_A(u_x(L)) - U_B(u_x(L)) + u_x(L)L) + (U'_A(u_x(L)) - U'_B(u_x(L)) + L)\epsilon + \dots > 0.$$

Because $u(x)$ is a solution to system (2.1), we have that $U_A(u_x(L)) + u_x(L)L = U_B(u_x(0))$. Thus, because ϵ is positive and arbitrarily small, for $\bar{\phi}$ to exist with the given restrictions, it is required that

$$U'_A(u_x(L)) - U'_B(u_x(L)) + L > 0.$$

The argument for the existence of sub- and supersolutions in other three cases is identical except for sign changes.

Because ϵ is arbitrarily small, the time-independent sub- and supersolutions are arbitrarily close to the steady state solutions $u(x)$. Therefore, based on the conditions for the existence of the sub- and supersolutions, the results presented in the previous section (inequalities (2.6) and (2.7)), and Proposition 3, the stability result is obtained.

The fact that the smaller of the two solutions is stable and the larger is unstable leads to the following interpretation. The “distance” of the stable solution from the unstable solution gives an idea of the size of the basin of attraction of the stable solution. In this light, the unstable solution acts as a threshold for jumping the gap, and one can begin to address the question of how noise or other perturbations could affect the signal blocking properties of the gap. That is, if a perturbation moves the solution $u(x, t)$ above the unstable steady state solution, then a wavefront forms on the distal side of the gap. (Note that a threshold result similar to that of Aronson and Weinberger [1] could be derived in which the perturbation need only make $u(x, t)$ sufficiently greater than the unstable steady state over a large enough region.)

3. Analogy to coupled cells. It was previously mentioned that the bifurcation parameter of interest is L/D when we are considering the existence of steady states. If $L \rightarrow 0$ with L/D constant, then we have the case of two identical excitable cables connected via an ohmic resistor. In many respects, this case is close to two excitable (bistable) cells coupled by a resistor of resistance $1/c_g$

$$(3.1) \quad \begin{cases} u'_1 &= f(u_1) + c_g(u_2 - u_1), \\ u'_2 &= f(u_2) + c_g(u_1 - u_2). \end{cases}$$

Indeed, under appropriate scaling, a finite cable with an inhomogeneity identical to the one considered here can be reduced to a pair of coupled cells [29].

The question that was considered for the full partial differential equation can also be considered for the case of the coupled cells: Assume that the two cells are at rest ($u_1 = 0, u_2 = 0$) and cell 2 receives a sufficiently large perturbation for it to become excited. Is the signal transmitted to cell 1 (i.e., does cell 1 become excited as well) or is the signal blocked?

In what follows, we show that the bifurcation structure of steady states in system (3.1) has the same qualitative features as the full gap model. Also, ordering principles can be derived for system (3.1) in a nearly identical way to those for the partial differential equation. Thus, the coupled cell problem (3.1) is analogous to the gap problem (1.1).

To see the similarity in bifurcation structure, the system is best studied in the u_2, u_1 -phase plane. Figures 3.1(a)–(c) show the phase planes for various values c_g in which a cubic f with $\alpha = 0.3$ is used. Figure 3.1(a) shows the phase plane for the

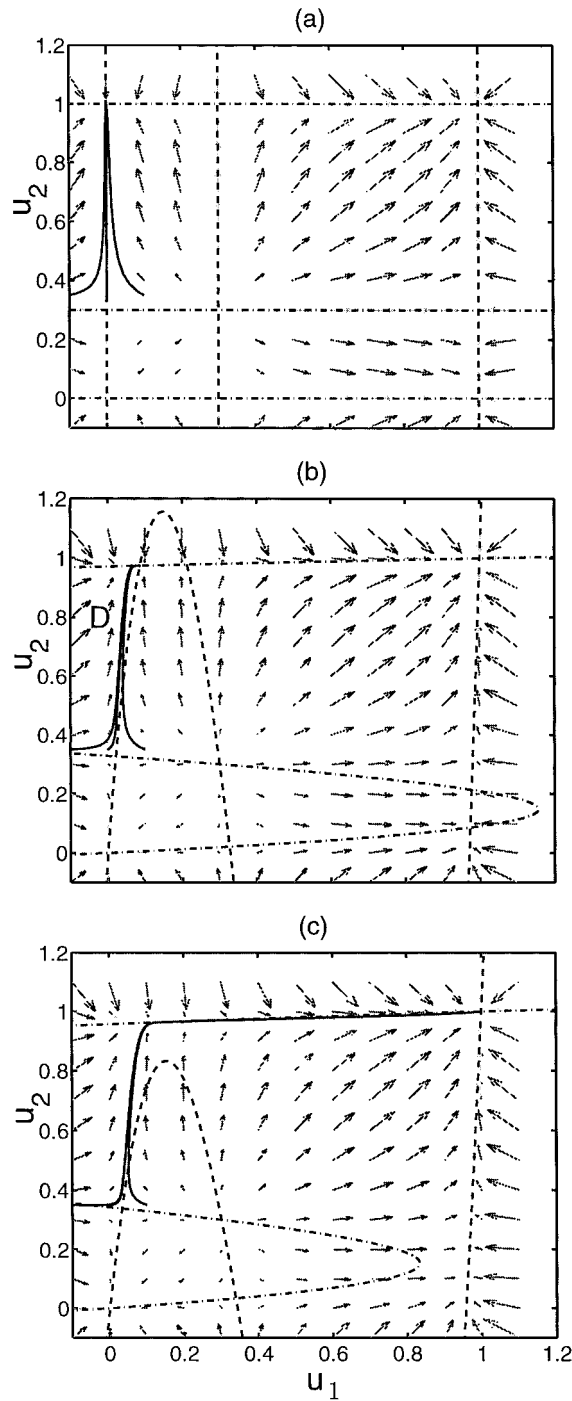


FIG. 3.1. Phase plane of coupled cells for cubic f with $\alpha = 0.3$. Dashed curves are portions of the u_1 -nullcline and the dash-dotted curves are portions of the u_2 -nullcline. A few trajectories are shown that begin at points corresponding to superthreshold perturbations of cell 2. (a) $c_g = 0$. The cells are uncoupled and therefore cell 1 does not become excited. (b) $c_g = 0.019$. The excitation signal is blocked, because the coupling is not sufficiently strong. (c) $c_g = 0.028$. Here, the coupling strength is large enough so that the excitation of cell 2 leads to the excitation of cell 1.

uncoupled case $c_g = 0$. There are nine steady states in all as seen by the intersections of the nullclines. The upper three, which have $u_2 = 1$, are of the most interest here. The steady state at $(u_1, u_2) = (0, 1)$ and $(1, 1)$ are stable nodes, which correspond to cell 2 being excited with cell 1 at rest and both cells being excited, respectively. The steady state at $(\alpha, 1)$ is a saddle point that separates the basins of attraction of the two stable nodes. If the cells are both at rest (i.e., at the stable node $(0, 0)$) and a perturbation is given to cell 2 that raises u_2 above α , cell 2 becomes excited and u_2 increases to 1. Cell 1, of course, remains unchanged at $u_1 = 0$. Thus, the signal is blocked.

For small c_g , this behavior persists. Of note, however, is the appearance of the full structure of the nullclines and the fact that the node that was at $(0, 1)$ and the saddle point that was at $(\alpha, 1)$ are shifted towards one another. This is seen in Figure 3.1(b), where $c_g = 0.019$. Sufficiently large perturbations of cell 2 away from $(0, 0)$ fall into a positively invariant region D (limited by the immediately surrounding nullclines). The flow in this region funnels all trajectories into the only stable point in the region, the stable node that was shifted from $(0, 1)$. Thus, the signal is still blocked.

As c_g is increased further, the stable node that was at $(0, 1)$ and the saddle that was at $(\alpha, 1)$ for the uncoupled system collide and vanish via a saddle-node bifurcation. For the case shown in the figures, this bifurcation point is at $c_g = 0.0235$. Following the bifurcation, the basin of attraction of the old stable steady state is absorbed by that of the steady state $(1, 1)$. Perturbations that excite cell 2 now lead to an excitation of cell 1 and the successful transmission of signal. This is seen in Figure 3.1(c), where $c_g = 0.028$.

Thus, we see the similarity between the coupled cell model and the gap problem. The saddle that was at $(\alpha, 1)$ in the uncoupled system is analogous to the unstable steady state solution of equation (1.1) and the stable node that was at $(0, 1)$ is analogous to the stable solution. Moreover, the transition between signal block and successfully signal transmission is associated with a saddle-node bifurcation. Thus, in retrospect, we should not be surprised by the bifurcation structure in the gap problem, because of its similarity to the very easily studied coupled cell system. Also, note that by changing the ‘‘diameter’’ of one of the cells instead of the coupling strength, this analogy can be extended to the case of an abrupt change in diameter of a cable.

4. Other gap dynamics. In this section, we extend results to include different gap dynamics and show that many qualitative features of the simple diffusive gap case carry over to more general gap dynamics.

4.1. Variable diffusion coefficient. The true parameter involved in determining the existence of steady state solutions to equation (1.1), and therefore wavefront block, is total resistance in the gap. Consider the case of a variable diffusion coefficient, $d(x)$, in the gap $0 < x < L$ and the excitable portion as originally defined. The matching conditions change slightly to

$$\begin{aligned} \lim_{x \rightarrow 0^-} u &= \lim_{x \rightarrow 0^+} u, & \lim_{x \rightarrow 0^-} u_x &= \lim_{x \rightarrow 0^+} d(0)u_x, \\ \lim_{x \rightarrow L^+} u &= \lim_{x \rightarrow L^-} u, & \lim_{x \rightarrow L^+} u_x &= \lim_{x \rightarrow L^-} d(L)u_x. \end{aligned}$$

Integrating the equation for gap dynamics,

$$\begin{aligned} (d(x)u_x)_x &= 0, \\ u_x(x) &= \frac{u_x(0)}{d(x)}, \end{aligned}$$

$$u(x) = u_x(0) \int_0^x [d(y)]^{-1} dy + u(0).$$

This results in a map

$$\psi_L : [u(0), u_x(0)] \mapsto \left[u_x(0) \int_0^L [d(x)]^{-1} dx + u(0), u_x(0) \right].$$

Thus we see that the total resistance $\int_0^L [d(x)]^{-1} dx$ determines the mapping of points on curve A through the gap to curve B .

This mapping implies that an asymmetric diffusion coefficient within the gap does not give rise to unidirectional block, i.e., it does not make it easier to block a wave traveling towards the gap in one direction compared to a wave traveling towards the gap in the other direction [18, 19, 26]. Unidirectional block can only occur when the two excitable regions of the cable have different diffusion coefficients. For a gap length of zero and only a change in diffusion coefficients, this situation would be equivalent to problems considered by Pauwelussen [30] (changing diameter of a neuron) and Fife and Peletier [9] (changing mobility in space). It should be noted that if the gap has nonzero excitability and D varies through the gap, then one-way block can occur [9].

4.2. Leaky gap. Similar analysis can be performed in the (perhaps more physical) case where gap dynamics include a leakage term, $-\gamma u$, in addition to diffusion:

$$u_t = Du_{xx} - \gamma u, \quad x \in (0, L).$$

Because only the dynamics in the gap are altered, only the map ψ_L is changed. The new map is

$$\begin{aligned} \tilde{\psi}_L : [u(0), u_x(0)] \mapsto & \left[\frac{u_x(0)}{\sqrt{D\gamma}} \sinh \sqrt{\frac{\gamma}{D}} L + u(0) \cosh \sqrt{\frac{\gamma}{D}} L, \right. \\ & \left. u_x(0) \cosh \sqrt{\frac{\gamma}{D}} L + Du(0) \sqrt{\frac{\gamma}{D}} \sinh \sqrt{\frac{\gamma}{D}} L \right]. \end{aligned}$$

It is easy to show that as $\gamma \rightarrow 0$, $\tilde{\psi}_L \rightarrow \psi_L$. However, for a sizeable leakage term, some results differ from the strictly diffusive case, as shown in Figures 4.1(a-d). The addition of this leakage term results in a lower critical gap length L^* as one should expect. It also allows for the possibility of nonmonotonic solutions (which are always unstable according to Sturm–Liouville theory [4]). Furthermore, for γ not too small, almost the entire function f is represented along solutions (i.e., very little of f is unimportant in determining block unlike the case with $\gamma = 0$). These differences are products of the new map having only one fixed point $(0,0)$ (rather than two) and lifting the rest of the homoclinic orbit including the point $(\alpha, 0)$ up towards the stable manifold of $(1,0)$.

Despite the difference in the map and solutions, the important aspects of the topology of the system remain the same as those for the strictly diffusive gap. Solutions arise via limit point bifurcations and super- and subsolutions solutions can be constructed in a similar manner as those in section 2.6, leading to stability results similar to the strictly diffusive case (see Figure 4.1(c)).

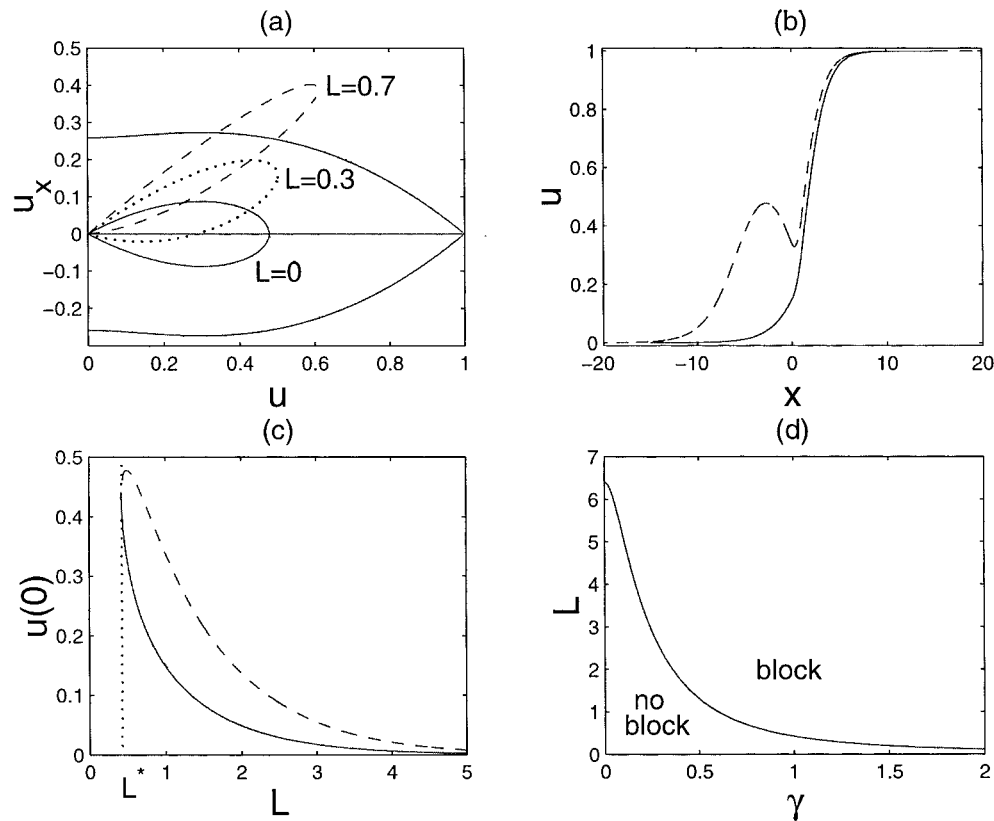


FIG. 4.1. (a) The u, u_x -phase portrait of $u_{xx} + f(u) = 0$ with images of the homoclinic orbit (curve A) under the map ψ_L for leaky gap. The first intersection is at $L^* = 0.426$. (b) The steady states for leaky gap at $L = 1.0$. The solid line represents the stable solution and the dashed line represents the unstable solution. (c) Bifurcation diagram for leaky gap: $u(0)$ of the steady state vs. gap length (L). The solid line represents stable solutions and the dashed line represents unstable solutions. The critical gap length is $L^* = 0.426$. (d) Critical gap length L^* vs. γ for leaky gap. (Locus of the fold.) This curve was calculated using AUTO [6]. $\alpha = 0.3$ and $D = 1$ in (a-d) and $\gamma = 1.0$ in (a-c).

4.3. Gap with low excitability. Regions of reduced excitability can also be addressed using the present analysis. Consider (1.1) with a local inhomogeneity described by

$$(4.1) \quad h(u, x) = \begin{cases} s(x)f(u), & 0 \leq x < L, \\ f(u) & \text{otherwise.} \end{cases}$$

We can generate a map under the flow of the gap dynamics, use this to map points on the homoclinic orbit determined by the outer equations and look for intersections of this mapped curve with the stable manifold of $(1,0)$. The only difference is that the map cannot be written explicitly and must be generated numerically. Examples of the mapping for constant s are shown in Figure 4.2(a), where L is varied, and Figure 4.2(b), where s is changed. Again, the major qualitative features are similar to those for the diffusive gap case. (For analytical estimates of critical gap length see [9, 27]).

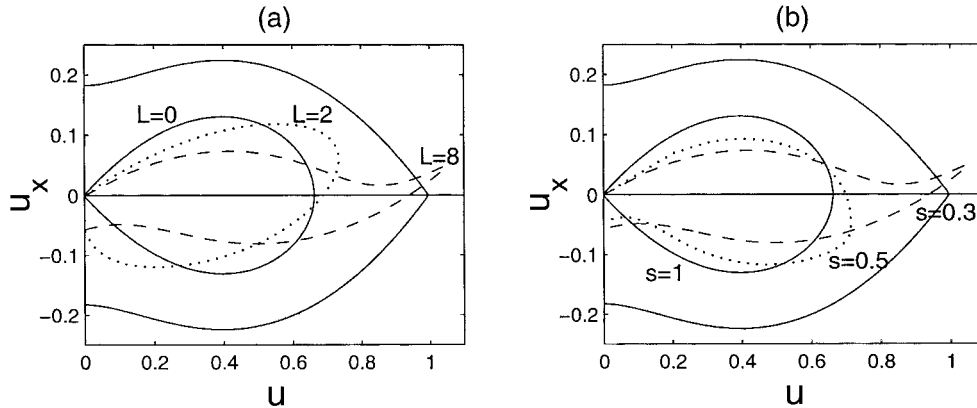


FIG. 4.2. The u, u_x -phase portrait of $u_{xx} + f(u) = 0$ with images of the homoclinic orbit under the map flow of $u_{xx} + sf(u) = 0$. (a) $\alpha = 0.4, s = 0.3$. (b) $\alpha = 0.4, L = 8.0$.

4.4. General gap dynamics. The geometric method that is used to find critical gap properties and steady state solutions in this paper is by no means limited to the cases presented. It can be applied to any problem which has a local inhomogeneity, and therefore the qualitative results obtained for the cases presented here carry over to the general case.

PROPOSITION 7. *Consider the scalar gap problem (1.1) with general gap dynamics ($g(u, x)$ integrable). As parameters are changed (perturbing the system away from the case of a uniform cable ($L = 0$)), the transition between successful propagation across the gap and block is associated with the birth of steady state solutions via a limit point bifurcation.*

This is a simple result of the topology of the problem and the proof is identical to the proof for the strictly diffusive gap (see Proposition 4) with one generalization. The map acting on curve A is defined by the flow in the gap. In general, the map must be numerically generated, as was the case in the previous section.

Note that the gap itself need not be homogeneous in order to apply the method. If dynamics in the gap are piecewise defined, then the full map can be obtained by convolving the piecewise defined maps. For general heterogeneous gap dynamics, the map is generated by solving the full nonhomogeneous ordinary differential equation describing steady state gap dynamics. In a similar fashion, the geometric method can be extended for use in finite and semi-infinite cables with either Neumann or Dirichlet boundary conditions.

In some ways this is a natural manifestation of the continuity properties of the equations and Proposition 3, because they imply that the only possible way nonuniform solutions with the appropriate boundary conditions can appear is via a limit point bifurcation.

5. Discussion. In this paper, we consider wavefront propagation and propagation failure in a spatially distributed scalar excitable medium that contains a local inhomogeneity. By quoting existing theorems, we describe the link between the existence of steady state solutions and the ability of the local inhomogeneity to block wavefront propagation. We then develop a geometric method that allows one to quickly and easily determine when these steady state solutions exist. Furthermore, this method immediately shows several important features of solutions and the overall

behavior of the problem. The simple case of a strictly diffusive gap is studied in detail, but we show that other local inhomogeneities have the same qualitative features as this simple case.

We find that block is associated with a limit point bifurcation. There exists a critical gap length L^* such that no solutions exist for $L < L^*$, exactly one solution exists for $L = L^*$, and two (or more) solutions exist for $L > L^*$. For $L > L^*$, we use upper and lower solution techniques to prove that the larger of the two solutions is unstable, whereas the smaller solution is stable. The unstable solution can be interpreted as a threshold for jumping the gap. If the solution is perturbed so that it lies above the (largest) unstable solution, the entire medium will become excited. The “distance” between the stable solution and the unstable solution provides a measure of the size of the basin of attraction of the stable solution (i.e., just how stable the stable solution is). The graphical representation of the problem also shows the important portions of the reaction term that determine whether or not block occurs. In the case of the strictly diffusive gap, when the system is highly excitable outside the gap, there is a sizable portion of f that plays no role whatsoever in the dynamics of wavefront block.

A reasonable conjecture is that block in nonuniform bistable excitable systems is always associated with limit point bifurcations. This is clearly demonstrated in the simple system of coupled excitable cells and is shown here for local gap inhomogeneities. It is also the case for bistable cables containing an abrupt change in parameters [30, 16], which is seen by overlaying the phase planes describing dynamics on either side of the abrupt change (see [30, Figure 10]). Furthermore, the association of block with a limit point has also been demonstrated in spatially distributed discrete reaction-diffusion equations [7, 3], and is implicitly suggested for periodically varying media (see equation (37) in [24]).

We believe the analysis and results presented here help to elucidate the problem of determining which properties regulate the ability of a wave of excitation to be transmitted across gaps of inexcitability or low excitability. This includes uncovering the dynamical structure underlying the behavior. However, because only the scalar system is considered, the direct applicability of this work to general excitable media needs further consideration. When recovery dynamics are included, the critical gap length that marks the transition from successful transmission of the signal through the gap to transmission block is modulated. For a large class of recovery dynamics, the critical gap length for the scalar problem serves as an upper bound to the critical gap length when recovery is included. The analysis presented here provides a good estimate for the critical gap length when the time scale of recovery is much larger than the characteristic times for diffusion in the gap and excitation. In this case, perturbation arguments allow one to study the effects of refractoriness on conditions for wave-block by considering slowly varying recovery variables as parameters (e.g., the changes of L^* due to changes in the threshold for local excitation can be thought of in this light; see Figure 2.6). We are in the process of performing a perturbation analysis in which we find that propagation failure in the system with recovery can be understood as slow capture near a limit point. This is analogous to previous work by Booth and Erneux in the spatially distributed discrete Fitzhugh–Nagumo equation [3].

Further complications arise when recovery dynamics are not an order of magnitude slower than excitability dynamics or when excitability cannot be described by a single variable. Most simple caricature models of the electrical activity in physio-

logical tissue do not have these problems. Generally, they have a single fast variable that is responsible for the autocatalytic process in excitation and fairly slow recovery variables. Therefore, if we implement these models in the gap problem, we can set the recovery variables to constants, apply perturbation methods and our geometric method, and confidently approximate the critical gap length. Unfortunately, more detailed models of cardiac and neural tissue have both several excitability variables and some fairly fast recovery variables (e.g., [15, 28, 2]). Thus, it is not easy to get good quantitative approximations of the critical gap length from a physiological standpoint. It may be possible that this can be overcome by deriving “effective” one-variable excitation terms for these detailed models. We have had some preliminary success in accomplishing this for a specific case (the Noble model [28]), but much more work needs to be done before a general method for this type of reduction can be attained.

REFERENCES

- [1] D. G. ARONSON AND H. F. WEINBERGER, *Nonlinear diffusion in population genetics, combustion and nerve pulse propagation*, in *Partial Differential Equations and Related Topics*, Lecture Notes in Math. 446, Springer-Verlag, New York, 1975, pp. 5–49.
- [2] G. W. BEELER AND H. REUTER, *Reconstruction of the action potential of myocardial fibres*, *J. Physiol.*, 268 (1977), pp. 177–210.
- [3] V. BOOTH AND T. ERNEUX, *Understanding propagation failure as a slow capture near a limit point*, *SIAM J. Appl. Math.*, 55 (1995), pp. 1372–1389.
- [4] E. A. CODDINGTON AND N. LEVINSON, *Theory of Ordinary Differential Equations*, McGraw-Hill, New York, 1955.
- [5] M. DELMAR AND J. JALIFE, *Wenckbach periodicity: From deductive electrocardiographic analysis to ionic mechanisms*, in *Cardiac Electrophysiology: From Cell to Bedside*, D. P. Zipes and J. Jalife, eds., W.B. Saunders, Philadelphia, PA, 1990, pp. 128–138.
- [6] E. J. DOEDEL, *AUTO, a program for the automatic bifurcation analysis of autonomous systems*, *Congr. Numer.*, 30 (1981), pp. 265–384.
- [7] T. ERNEUX AND G. NICOLIS, *Propagation waves in discrete bistable reaction-diffusion systems*, *Phys. D*, 67 (1993), pp. 237–244.
- [8] P. C. FIFE AND J. B. MCLEOD, *The approach of solutions of nonlinear diffusion equations to traveling front solutions*, *Arch. Rat. Mech. Anal.*, 65 (1977), pp. 335–361.
- [9] P. C. FIFE AND L. A. PELETIER, *Clines induced by variable selection and migration*, *Proc. R. Soc. London Ser. B*, 214 (1981), pp. 99–123.
- [10] R. A. FISHER, *The wave advance of advantageous genes.*, *Ann. Eugen.*, 7 (1937), pp. 355–369.
- [11] S. S. GOLDSTEIN AND W. RALL, *Changes of action potential shape and velocity for changing core conductor geometry*, *Biophys. J.*, 14 (1974), pp. 731–757.
- [12] M. R. GUEVARA, *Spatiotemporal patterns of block in an ionic model of cardiac Purkinje fibre*, in *From Chemical to Biological Organization*, M. Markus, S. Muller, and G. Nicolis, eds., Springer-Verlag, Berlin, 1988, pp. 273–281.
- [13] T. D. HASSINGER, P. B. GUTHERIE, P. B. ATKINSON, M. V. L. BENNETT, AND S. B. KATER, *An extracellular signaling component in propagation of astrocytic calcium waves*, *Proc. Natl. Acad. Sci. USA*, 93 (1996), pp. 13268–13273.
- [14] M. HINES, *Efficient computation of branched nerve equations*, *Int. J. Biomed. Comput.*, 15 (1984), pp. 69–76.
- [15] A. L. HODGKIN AND A. F. HUXLEY, *A quantitative description of membrane current and its application to conduction and excitation in nerve*, *J. Physiol.*, 117 (1952), pp. 500–544.
- [16] H. IKEDA AND M. MIMURA, *Wave-blocking phenomena in bistable reaction-diffusion systems*, *SIAM J. Appl. Math.*, 49 (1989), pp. 515–538.
- [17] J. JALIFE, *The sucrose gap preparation as a model of AV nodal transmission: Are dual pathways necessary for reciprocation and AV nodal echos?*, *Pacing and Clinical Electrophysiology*, 6 (1989), pp. 1106–1122.
- [18] M. J. JANSE, *Reentry rhythms*, in *The Heart and Cardiovascular System*, H. Fozzard, E. Harber, R. Jennings, A. Katz, and H. Morgan, eds., Raven Press, New York, 1986, pp. 1203–1238.
- [19] R. W. JOYNER, *Mechanisms of unidirectional block in cardiac tissues*, *Biophys. J.*, 35 (1981), pp. 113–125.

- [20] A. M. KATZ, *Physiology of the Heart*, 2nd ed., Raven Press, New York, 1992.
- [21] J. P. KEENER, *On cardiac arrhythmias: AV conduction block*, J. Math. Biol., 12 (1981), pp. 215–225.
- [22] J. P. KEENER, *Dynamic patterns in excitable media*, in Modelling of Patterns in Space and Time, Lecture Notes in Bio. Math. 55, S. Levin, ed., Springer-Verlag, Berlin, 1984, pp. 157–169.
- [23] J. P. KEENER, *Propagation and its failure in coupled systems of discrete excitable cells*, SIAM J. Appl. Math., 47 (1987), pp. 556–572.
- [24] J. P. KEENER, *Homogenization and propagation in the bistable equation*, Phys. D, 136 (2000), PP. 1–17.
- [25] H. KELLER, *Numerical Methods for Two-Point Boundary Value Problems*, Ginn (Blaisdell), Boston, 1968.
- [26] M. LEWIS AND P. GRINDROD, *One-way block in cardiac tissue: A mechanism for propagation failure in Purkinje fibres*, Bull. Math. Biol., 53 (1991), pp. 881–899.
- [27] T. J. LEWIS, *Signal Propagation in Inhomogeneous Excitable Media: Propagation Failure and Reflection*, Ph.D. thesis, University of Utah, Salt Lake City, UT, 1998.
- [28] D. NOBLE, *A modification of the Hodgkin-Huxley equations applicable to Purkinje fiber action and pacemaker potential*, J. Physiol., 160 (1962), pp. 317–352.
- [29] H. G. OTHMER, *A continuum model for coupled cells*, J. Math. Biol., 17 (1983), pp. 351–369.
- [30] J. P. PAUWELUSSEN, *Nerve impulse propagation in a branching nerve system: A simple model*, Phys. D, 4 (1981), pp. 67–88.
- [31] J. P. PAUWELUSSEN, *One way traffic of pulses in a neuron*, J. Math. Biol., 15 (1982), pp. 151–171.
- [32] M. H. PROTTER AND H. F. WEINBERGER, *Maximum Principles in Differential Equations*, Springer-Verlag, New York, 1984.
- [33] F. RAMON, R. W. JOYNER, AND J. W. MOORE, *Propagation of action potentials in inhomogeneous axon regions*, Federation Proc., 34 (1975), pp. 1357–1363.
- [34] G. J. ROZANSKI, J. JALIFE, AND G. K. MOE, *Reflected reentry in nonhomogenous ventricular muscle as a mechanism of cardiac arrhythmias*, Circulation, 69 (1984), pp. 163–173.
- [35] G. H. SHARP AND R. W. JOYNER, *Simulated propagation of the cardiac action potentials*, Biophys. J., 31 (1980), pp. 403–423.
- [36] J. SNEYD AND J. SHERRATT, *On the propagation of calcium waves in an inhomogeneous medium*, SIAM J. Appl. Math., 57 (1997), pp. 73–94.
- [37] P. A. SPIRO, *Mathematical Studies of Cell Signal Transduction*, Ph.D. thesis, University of Utah, Salt Lake City, UT, 1997.
- [38] J. X. XIN AND J. ZHU, *Quenching and propagation of bistable reaction-diffusion fronts in multidimensional periodic media*, Phys. D, 81 (1995), pp. 94–110.
- [39] A. XU AND M. R. GUEVARA, *Two forms of spiral-wave reentry in an ionic model of ischemic ventricular myocardium*, Chaos, 8 (1998), pp. 157–174.
- [40] Y. ZHOU AND J. BELL, *Study of propagation along nonuniform excitable fibers*, Math. Biosci., 119 (1994), pp. 169–203.